EuroIntervention 2021;17:e1009-e1018 published online July 2021 ■ published online e-edition December 2021

Chronic haemodynamic performance of a biorestorative transcatheter heart valve in an ovine model

Patrick W. Serruys[1,2,3]*, MD, PhD; Hideyuki Kawashima[1,4], MD; Chun-Chin Chang[5], MD; Rodrigo Modolo[4,6], MD; Rutao Wang[1,7], MD; Robbert J. de Winter[4], MD, PhD; Hadewych Van Hauwermeiren[8], DVM, MLAS; Mohammed El-Kurdi[9], PhD; Wian van den Bergh[9], MSc; Martijn Cox[9], PhD; Yoshinobu Onuma[1], MD, PhD; Willem Flameng[10], MD, PhD; Osama Soliman[1,2], MD, PhD

1. Department of Cardiology, National University of Ireland, Galway (NUIG) and CORRIB Corelab and Center for Research and Imaging, Galway, Ireland; 2. CÚRAM, the SFI Research Centre for Medical Devices, Galway, Ireland; 3. NHLI, Imperial College London, London, United Kingdom; 4. Department of Cardiology, Academic Medical Centre, University of Amsterdam, Amsterdam, the Netherlands; 5. Division of Cardiology, Department of Internal Medicine, Taipei Veterans General Hospital, National Yang Ming University, Taipei, Taiwan; 6. Department of Internal Medicine, Cardiology Division, University of Campinas (UNICAMP), Campinas, Brazil; 7. Department of Cardiology, Radboud University Medical Center, Nijmegen, the Netherlands; 8. Medanex Clinic B.V., Preclinical CRO, Diest, Belgium; 9. Xeltis B.V., Eindhoven, the Netherlands; 10. Department of Cardiac Surgery, Katholieke Universiteit (K.U) Leuven, Leuven, Belgium

P.W. Serruys and H. Kawashima share equal first authorship.

This paper also includes supplementary data published online at: https://eurointervention.pcronline.com/doi/10.4244/EIJ-D-21-00386

KEYWORDS

- innovation
- preclinical research
- TAVI

Abstract

Background: The Xeltis biorestorative transcatheter heart valve (BTHV) leaflets are made from an electrospun bioabsorbable supramolecular polycarbonate-urethane and are mounted on a self-expanding nitinol frame. The acute haemodynamic performance of this BTHV was favourable.

Aims: We sought to demonstrate the preclinical feasibility of a novel BTHV by evaluating the haemodynamic performances of five pilot valve designs up to 12 months in a chronic ovine model.

Methods: Five design iterations (A, B, B', C, and D) of the BTHV were transapically implanted in 46 sheep; chronic data were available in 39 animals. Assessments were performed at implantation, 3, 6, and 12 months including quantitative aortography, echocardiography, and histology.

Results: At 12 months, greater than or equal to moderate AR on echocardiography was seen in 0%, 100%, 33.3%, 100%, and 0% in the iterations A, B, B', C, and D, respectively. Furthermore, transprosthetic mean gradients on echocardiography were 10.0±2.8 mmHg, 19.0±1.0 mmHg, 8.0±1.7 mmHg, 26.8±2.4 mmHg, and 11.2±4.1 mmHg, and effective orifice area was 0.7±0.3 cm^2, 1.1±0.3 cm^2, 1.5±1.0 cm^2, 1.5±0.6 cm^2, and 1.0±0.4 cm^2 in the iterations A, B, B', C, and D, respectively. On pathological evaluation, the iteration D demonstrated generally intact leaflets and advanced tissue coverage, while different degrees of structural deterioration were observed in the other design iterations.

Conclusions: Several leaflet material iterations were compared for the potential to demonstrate endogenous tissue restoration in an aortic valve *in vivo*. The most promising iteration showed intact leaflets and acceptable haemodynamic performance at 12 months, illustrating the potential of the BTHV.

**Corresponding author: Department of Cardiology, National University of Ireland Galway (NUIG) and CORRIB Corelab and Centre for Research and Imaging, University Road, Galway, H91 TK33, Ireland. E-mail: patrick.w.j.c.serruys@gmail.com*

SUBMITTED ON 26/04/2021 - REVISION RECEIVED ON 1st 15/05/2021 / 2nd 04/07/2021 - ACCEPTED ON 15/07/2021

DOI: 10.4244/EIJ-D-21-00386

Abbreviations

AR	aortic regurgitation
BTHV	biorestorative transcatheter heart valve
EOA	effective orifice area
ETR	endogenous tissue restoration
PG	pressure gradients
SVD	structural valve deterioration
TAVI	transcatheter aortic valve implantation
UPy	ureidopyrimidinone
VD-AR	videodensitometric aortic regurgitation

Introduction

The recent approval of transcatheter aortic valve implantation (TAVI) for patients at low operative risk, based on the results of the randomised PARTNER 3[1] and Evolut Low Risk[2] trials, has opened a new avenue of wider TAVI expansion into lower surgical risk and younger populations as well as the introduction of novel and potentially improved technologies into patient care. However, the midterm and long-term durability of bioprosthetic valves remains a major concern, especially for patients with longer life expectancy[3].

Tissue-engineered heart valves aim to address this unmet need for long-lasting bioprosthetic valve replacement by ultimately providing patients with a regenerated autologous valve[4-6]. Various tissue engineering concepts have been brought forward, often including extensive periods of *ex vivo* cell manipulation and tissue culture. Most progress has been made in the low-pressure system, where encouraging sheep data have been reported up to one year[7,8], although Syedain et al reported promising six-month follow-up in an ovine surgical aortic valve model[9]. No reports were found on chronic follow-up with a transcatheter valve in a systemic model[10]. Translation to clinical applications has thus far been lacking, possibly hampered by the complexity and costs associated with the required manufacturing processes. More recently, endogenous tissue restoration (ETR) has emerged as an alternative approach that does not require *ex vivo* cell manipulation. The fundamental concept of an ETR-based valve is that bioprosthetic leaflets made from bioabsorbable material will be progressively replaced by endogenous tissue[4-6]. The potential advantages of ETR include dry storage, scalable production and predictable manufacturing. Promising preclinical data in various low-pressure applications[11-15] have paved the way for clinical evaluation of this approach, and several clinical trials are now ongoing[16,17].

The Xeltis biorestorative transcatheter heart valve (BTHV; Xeltis BV, Eindhoven, the Netherlands) showed salient haemodynamic performance, with an acceptable aortic regurgitation (AR) immediately after TAVI in a preclinical study[18]. In this preclinical study, we sought to report the chronic haemodynamic performance of the BTHV in an ovine aortic valve model.

Methods

STUDY DESCRIPTION

The detailed study design has been described previously[18]. In brief, this preclinical study included 46 Ile de France sheep (age: 9-12 months, weight: 40-60 kg) that received BTHV implantation. All BTHVs had a uniform diameter of 26 mm and were implanted in native annuli with an approximate diameter of 23 mm as confirmed by an echocardiographic pre-screening. Therefore, sizing/light oversizing (26 mm BTHV) was uniformly applied in all animals. TAVI was performed via transapical approach with a 24 Fr delivery system. After TAVI, study animals were monitored, and euthanasia, necropsy and subsequent histopathology were scheduled at 3, 6, or 12 months. The study protocol adhered to the Directive 2010/63/EU of the European Parliament and of the Council of 22 September 2010 on the protection of animals used for scientific purposes and the Guide for the Care and Use of Laboratory Animals and was reviewed and approved by the Test Facility's Ethical Committee for compliance with regulations prior to study initiation.

DESIGN OF THE XELTIS BTHV

The leaflets of the Xeltis BTHV are made from a bioabsorbable supramolecular polycarbonate urethane based on the ureidopyrimidinone (UPy) binding motif[19,20], which was electrospun into a tubular scaffold[4,14,18]. The tube was then formed into a heart valve by mounting on a uniformly self-expanding nitinol stent that included three feelers and three native leaflet clipping mechanisms. In this preclinical study, five leaflet iterations were tested **(Central illustration)**. Material iterations consist of various polymers (same building blocks, varying stoichiometry), different leaflet thickness (300 or 500 µm) and heterogeneous or homogeneous fibre orientation (random or aligned) **(Central illustration)**.

TAVI PROCEDURE

Implantation of the Xeltis BTHV has been described previously[18], and is also described in the extended methods section of **Supplementary Appendix 1**.

AORTOGRAPHIC ASSESSMENT OF AORTIC REGURGITATION

Aortography was performed according to a pre-specified protocol immediately after TAVI (acute phase)[18] and before scheduled euthanasia (chronic phase). The details of the acquisition and analysis of quantitative videodensitometric angiographic assessment of AR have been reported previously[21,22]. The following parameters were assessed on aortography: 1) AR severity and 2) aortic valve stent post deflection.

AORTIC REGURGITATION SEVERITY ASSESSMENT

AR severity was quantified in regurgitation fraction (videodensitometric aortic regurgitation, VD-AR) and the values were converted into scales of severity as less than mild (<6%), mild to moderate (6% to 17%), and moderate or more (>17%)[21,22]. In a binary fashion, we described VD-AR values as significant (>17%) and non-significant (≤17%). A dedicated software (CAAS A-Valve 2.0.2; Pie Medical Imaging, Maastricht, the Netherlands) was used to quantify AR severity from aortography DICOM films. Aortographic data were analysed in an independent core laboratory (CORRIB Research Centre for Advanced Imaging and

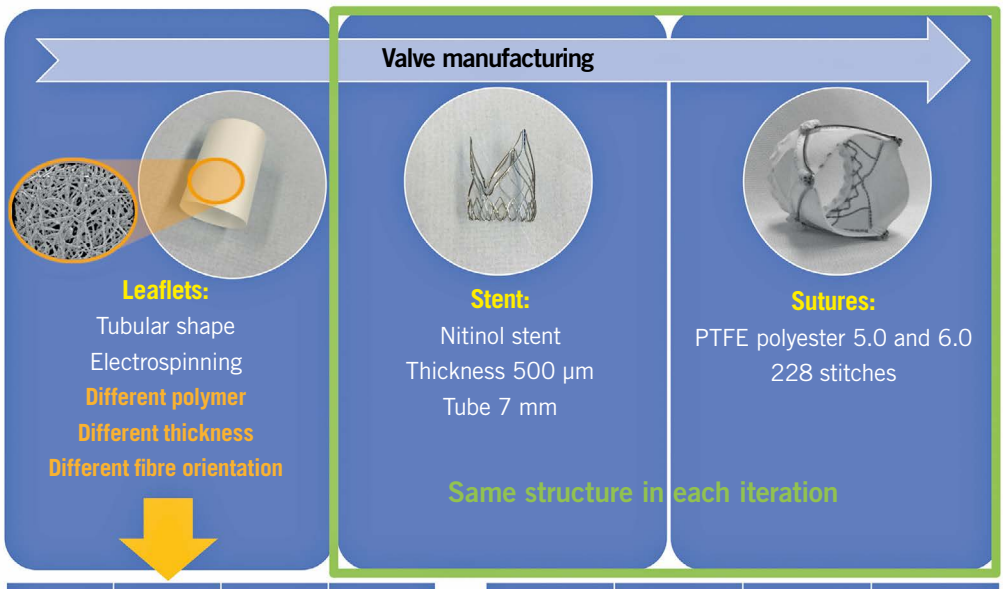

Iterations	Polymer	Thickness (µm)	Fibre orientation
A	a	500	Random
B	b	500	Aligned
B'	c	500	Random
C	a	300	Aligned
D	d	500	Random

Polymer	Mass% Soft block (PC)	Mass% Hard block (UPy part)	Bulk stiffness (MPa)
a	48	52	170
b	65	35	40
c	52	48	55
d	49	51	115

Central illustration. *Xeltis BTHV manufacturing. Leaflets with a porous microstructure made through the electrospinning process were mounted on a self-expanding nitinol frame that included three feelers and a native leaflet clipping mechanism. Electron microscopic images of the product of electrospinning (orange circle). BTHV: biorestorative transcatheter heart valve; PTFE: polytetrafluoroethylene*

Core Lab, Galway, Ireland) by experienced analysts who were blinded to other imaging data and anatomo-pathological results.

FLUOROSCOPIC ASSESSMENT OF STENT FRAME AND PINWHEELING

Due to the observation of pinwheeling phenomenon in some animals, we performed a *post hoc* analysis of aortic valve stent post deflection and pinwheeling effect on the leaflets in all animals. The detailed methodology and results of the analysis are described in the extended methods and results **(Supplementary Figure 1, Supplementary Table 1)** sections of **Supplementary Appendix 1** and **Supplementary Appendix 2**.

ECHOCARDIOGRAPHIC ACQUISITION AND ANALYSIS

All animals underwent serial echocardiography follow-up according to a pre-specified protocol in the Animal Test Facility (IMMR, Paris, France). Transthoracic echocardiography was performed at the following time points: preoperative, weekly after the procedure for one month, monthly thereafter and before scheduled euthanasia. Echocardiographic data were analysed in an independent core laboratory (CORRIB Research Centre for Advanced Imaging and Core Lab, Galway, Ireland) by experienced analysts who were blinded to other imaging data and anatomo-pathological results. The grade of AR severity (transvalvular, commissural, or paravalvular) as well as transvalvular mean and peak pressure gradients (PG), and effective orifice area (EOA) of the prosthetic aortic valve were analysed in accordance with published guidelines[23]. AR severity after the BTHV implantation was graded on echocardiography. The following AR severity grades were considered: less than mild regurgitation, mild regurgitation, moderate regurgitation, and severe regurgitation[24]. Significant prosthetic aortic stenosis was defined as a transvalvular mean PG ≥20 mmHg[24]. Furthermore, a reduction of EOA ≤0.9 cm^2 was judged as prosthetic valve dysfunction[24].

ANATOMO-PATHOLOGICAL EVALUATION

Pathological evaluation included gross examination and histology. Three leaflets were cut longitudinally and sections of each leaflet including the adjacent aortic root were assessed for histology. Tissues were dehydrated and embedded in paraffin. Sections were cut at 4 to 6 microns and stained with haematoxylin-eosin (H&E), Movat pentachrome (MP) stains, and Von Kossa stain for calcium. As shown on **Figure 1**, the thickness of the leaflet was measured at the base, at the middle, and at the free edge. The leaflet thickness score, thrombus score, collagen deposition score, matrix absorption score, and inflammation score were also calculated at the base, middle, and tip of the leaflet. The details of the calculations are described in the extended methods section of **Supplementary Appendix 1**.

In addition, radiographic (Faxitron) images were obtained to evaluate leaflet integrity and structure. Leaflets were examined on gross

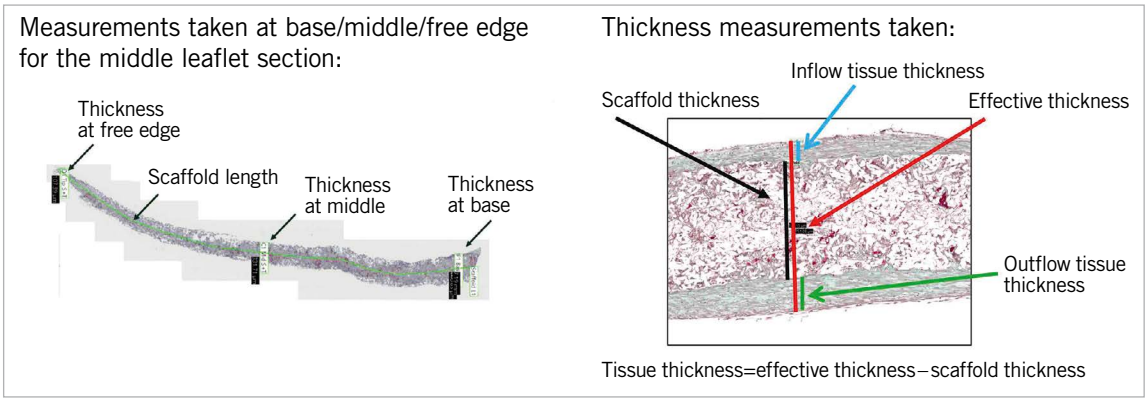

Figure 1. *Histological quantification of tissue thickness of the leaflet. Tissue thickness was quantified by effective thickness minus scaffold thickness of the leaflet. The thickness of the leaflet was measured at the base, middle, and tip (free edge). Furthermore, the length of the scaffold was measured. Thickness of the leaflet was quantified as the scaffold thickness and the effective thickness including the covering tissue. The tissue thickness was quantified using the following formula: the effective thickness - scaffold thickness.*

pathology for the presence or absence of tear by visual inspection and corroborated on radiographic images **(Supplementary Figure 2)**.

STATISTICAL ANALYSIS

Quantitative variables are reported as mean±standard deviation or median (interquartile range, 25-75%) as appropriate. Categorical variables are expressed as numeric values and percentages.

Results

STUDY ANIMALS

The BTHV was implanted in the native aortic annulus using a transapical approach in 46 animals. Overall, 39 animals survived to their intended time points, while 7 died before scheduled euthanasia **(Figure 2)**. The results of VD-AR following TAVI and before euthanasia and echocardiographic analysis at 7-day, 3-month, 6-month, and 12-month follow-up among the five BTHV design iterations are summarised in **Supplementary Table 2**.

TIME COURSE OF AR SEVERITY ON AORTOGRAPHY

VD-AR was analysable in 34 animals following TAVI (acute phase) and in 36 animals before euthanasia (chronic phase) **(Supplementary Figure 3, Supplementary Table 2)**. None of the animals presented with significant AR (>17% on VD-AR) on aortography in the acute phase, except one animal in each of the iterations B and C. There was no animal with significant VD-AR at three months.

The mean VD-AR at implantation, 3, 6, and 12 months among the five design iterations is presented in **Figure 3**. At 12 months, VD-AR was 8.0±9.9%, 65.7±19.3%, 24.3±11.0%, 38.7±23.9%, and 9.7±9.0% in the iterations A, B, B', C, and D, respectively.

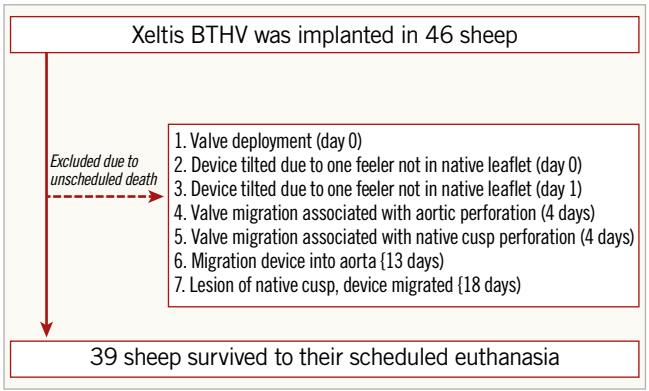

Figure 2. *Flow chart of the present study.*

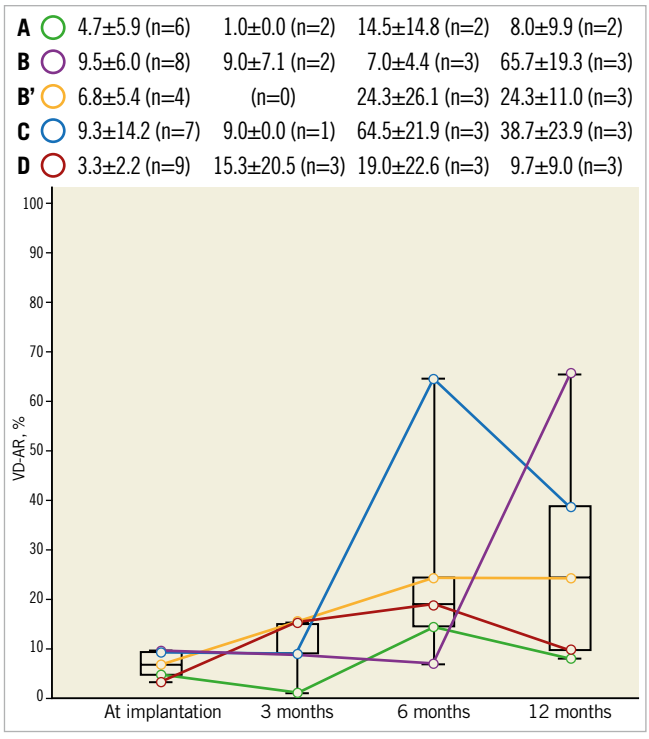

Figure 3. *Mean VD-AR at implantation, 3, 6, and 12 months among the five design iterations. Data are shown as mean±standard deviation or % (numbers). VD-AR: videodensitometric aortic regurgitation*

AORTIC REGURGITATION FINDING AND HAEMODYNAMICS ON ECHOCARDIOGRAPHY

The quantitative assessments of echocardiographic analysis are summarised in **Figure 4** and **Supplementary Table 2**. In iteration C, 12.5% of the animals demonstrated significant (≥moderate) AR on echocardiography at 3 months. On 6-month echocardiography, significant AR was seen in 25.0%, 0%, 0%, 16.7%, and 0% in the iterations A, B, B', C, and D, respectively. On 12-month echocardiography, significant AR was seen in 0%, 100%, 33.3%, 100%, and 0% in the iterations A, B, B', C, and D, respectively.

As shown in **Figure 4**, iteration C had ≥moderate AR in all animals associated with an increased transvalvular gradient (mean PG on

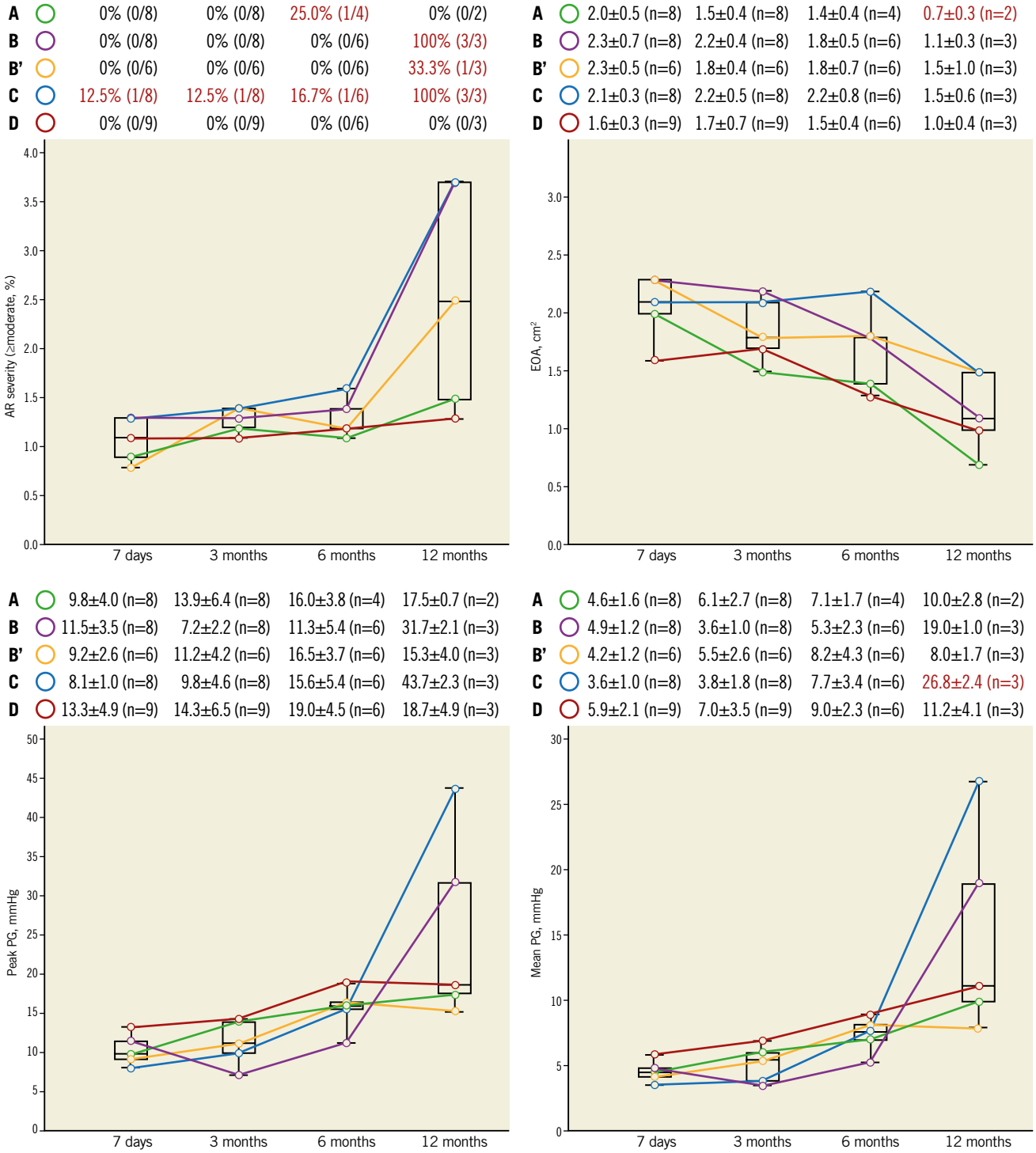

Figure 4. *Summary of echocardiographic assessments among the five design iterations. Data are shown as mean±standard deviation or % (numbers). Values presented in red text are considered as abnormal. AR: aortic regurgitation; EOA: effective orifice area; PG: pressure gradient*

average: 26.8±2.4 mmHg), suggestive of a prosthetic valve dysfunction at 12-month follow-up. Furthermore, iteration A had a prosthetic valve dysfunction at 12 months (EOA on average: 0.7±0.3 cm^2).

Supplementary Table 3 presents the different types (transvalvular, commissural, or paravalvular) of AR severity on echocardiography among the five design iterations. Greater than or equal to moderate – paravalvular – AR was not seen up to 12 months.

GROSS ANATOMO-PATHOLOGICAL INSPECTION OF LEAFLET

LEAFLET AND SCAFFOLD THICKNESS MEASUREMENTS

The median inflow and outflow tissue thickness at the base, middle, and tip (free edge) were measured at 3, 6, and 12 months post TAVI **(Figure 5)**. Overall, the results of histological measurements demonstrated that tissue thickness at the base of the leaflet was greater than at the middle or the free edge of the leaflet. Furthermore, the tissue coverage of the outflow side was better than the inflow side. The other results are described in the extended results section of **Supplementary Appendix 2**.

PATHOLOGICAL SCORES

Detailed scores of the neointimal thickness, thrombus, collagen deposition, matrix absorption, inflammation, and calcification scores of iterations D at 3-, 6-, and 12-month follow-up are presented in **Figure 6**. Those of the other four iterations are presented in **Supplementary Figure 4**. More profound host device interaction in the form of neointimal thickness, thrombus, collagen deposition, matrix absorption, inflammation, and calcification was observed at the base, middle, and tip parts of the leaflet. These changes were seen very early following the BTHV implantation using different iterations. Notably, collagen deposition (base: median score 2, 2, and 3 at 3, 6, and 12 months, respectively) and matrix absorption (base: median score 2, 3, and 3 at 3, 6, and 12 months, respectively) throughout the base, middle, and tip of the leaflet progressively increased over time in iteration D.

LEAFLET INTEGRITY ASSESSMENT ON RADIOGRAPHIC IMAGES

Leaflet gross pathology was classified into two categories (1: no tear, 2: tear) by visual inspection and corroborated on radiographic images **(Supplementary Figure 5)**. Overall, iteration D came out best, showing a tear in only 1 of 9 animals.

Discussion

In the present study, we investigated the feasibility of a BTHV using different iterations of the Xeltis BTHV **(Central illustration)**. The main findings of this study can be summarised as follows: 1) despite favourable acute performance of all five designs, the frame design may have compromised long-term durability in several designs; 2) one configuration, D, demonstrated adequate valve performance up to one year; 3) the histological data showed that tissue grew from the base to the tip and that tissue grew more in the outflow side compared to the inflow side. Collagen deposition and matrix absorption progressed with time from the base to the tip and were observed from three months following TAVI in iteration D. These findings represent an important step in the field of heart valve tissue engineering.

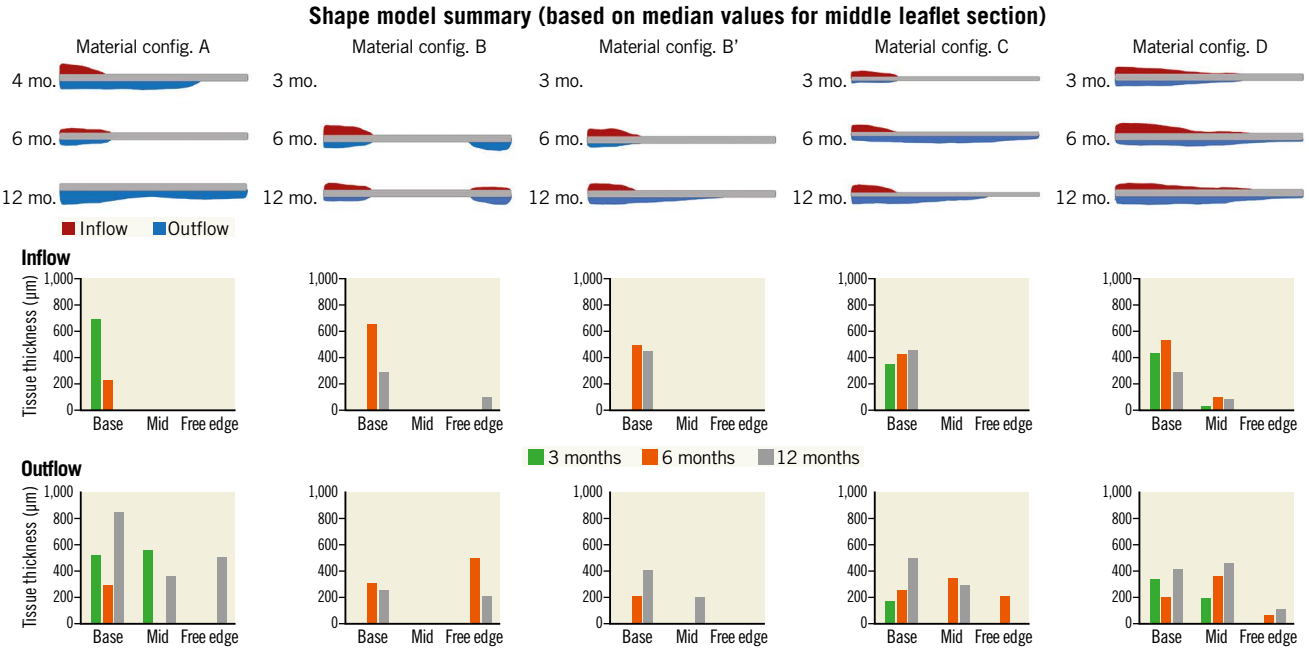

Figure 5. *Histological measurements of tissue coverage and tissue thickness. In the top of the panel, tissue thickness at the base of the leaflet (base) was thicker than at the middle (mid) or the tip of the leaflet (free edge) in the five iterations. Red colour represents the tissue coverage of the inflow side. Blue colour represents the tissue coverage of the outflow side. The middle of the panel: inflow tissue thickness (µm) of the five iterations. The bottom of the panel: outflow tissue thickness (µm) of the five iterations.*

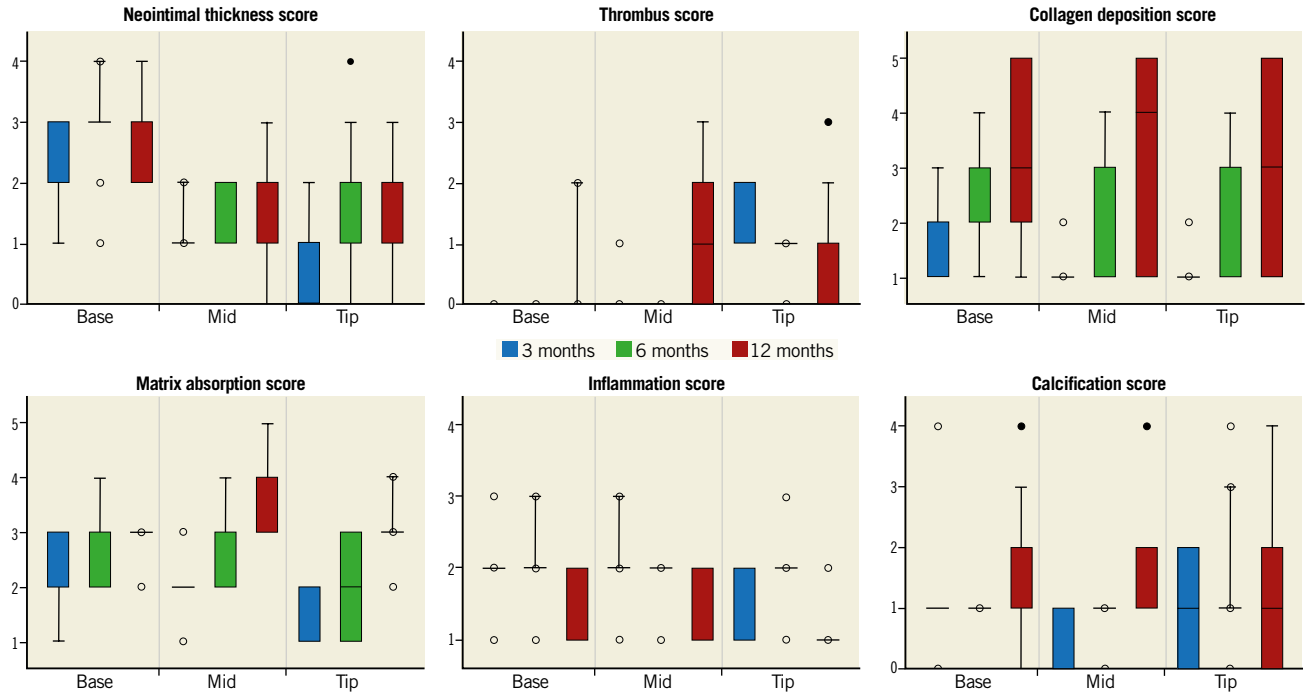

Figure 6. *Results of each pathological score in iteration D. Box-whisker plots of the neointimal thickness, thrombus, collagen deposition, matrix absorption, inflammation, and calcification scores at the base, middle, and tip of iteration D at 3-, 6-, and 12-month follow-up are presented. The upper and lower boundaries of the box represent the 75th and 25th percentiles, respectively. Whiskers above and below the box indicate the maximum and minimum values, respectively. The line within the box marks the median. Outliers are drawn as filled in circles. An outlier is a value that is larger than 1.5 times the IQR from the median. IQR is the difference between the first and third quartiles. The whiskers are only drawn to the smallest/largest non-outlier. Extreme outliers that are three times the IQR are drawn as open circles. IQR: interquartile range*

A PERFECT BIOPROSTHETIC AORTIC VALVE

Aortic valve replacement using a bioprosthesis has been used to treat patients with aortic stenosis or AR for several decades. One of the major limitations in the valve design is the leaflet material, typically manufactured from bovine or porcine material. The average lifespan of a bioprosthetic valve is estimated to be 15 years in elderly patients. In contrast, structural valve deterioration (SVD) is accelerated in younger patients due to a more pronounced immunologic response and enhanced calcification of the valve[25-27]. Bourguignon et al found that the expected valve durability (median survival time without SVD) was 17.6 years for the younger (≤60) group and 22.1 years for the 60 to 70 years group[28].

The expansion of TAVI into a younger population will require more durable valve designs to ascertain event-free survival that matches life expectancy. An ideal THV should be biologically compatible with the host and biologically stable, which means less susceptibility to thrombosis, structural degeneration, calcification, or pannus formation. Furthermore, the biomechanical strength of the valve design should avoid tear and allow a durability comparable to the host's life expectancy.

Several attempts at creating a life-lasting leaflet have been made. Indeed, many advances in materials science and the manufacturing process of mechanical or bioprosthetic valves have been tested previously in the clinical setting. However, the Ross procedure with cryopreserved or decellularised pulmonary homografts remains the gold standard in young adult patients. Nevertheless, it is surmised that novel artificial heart valves will involve electrospinning, polymeric materials, moulding, and additive manufacturing processes for the fabrication of customised heart valves.

The leaflets of the Xeltis BTHV are constructed by electrospinning **(Central illustration)**[4,14,18]. Electrospinning is a widely used technique for the electrostatic production of nanofibres, during which electric power is used to make polymer fibres with diameters ranging from 2 nm to several micrometres from polymer solutions or melts. This process is a major focus of attention because of its versatility and ability to produce fibres continuously on a scale of nanometres, which is difficult to achieve using other standard technologies. Electrospinning is a relatively simple way of creating nanofibre materials, but there are several parameters that can significantly influence the formation and structure of produced nanofibres. These parameters include solution variables, needle variables or collector variables, which could be manipulated to produce the desired material. In addition, the polymers a, b, c, and d are part of the same proprietary class of polycarbonates based on the supramolecular UPy binding motif **(Central illustration)**. These differ in the composition and stoichiometry of their building blocks. However, our current data do not provide sufficient mechanistic insights into why the iteration D and/or polymer d appear to be favourable in the chronic performance of the BTHV.

ITERATION D: PROMISING PROOF OF FEASIBILITY

To the best of our knowledge, this is the first study to report 12-month results of transapical prosthetic aortic valve implantation in sheep. Therefore, the rate of analysable animals at their intended time points (39/46 cases; 85%) should be considered acceptable. To date, preclinical TAVI models are simply not well established, in particular with commercially available valve designs.

Among the five designs, iteration D had the best performance in terms of haemodynamic performance and AR severity on aortography and echocardiography up to 12-month follow-up following TAVI. Furthermore, the mean transvalvular gradient in iteration D was comparable to commercially available valves. These data are supported by the histological findings. Iteration D demonstrated a better tissue coverage and a higher tissue thickness than the other iterations. Since a uniform stent platform was used in the valve design, the difference in tissue growth among the five iterations would be related mainly to the material of the leaflet. Notably, the tip (free edge) of the leaflets was not fully covered by tissue at 12 months in all the iterations, especially at the inflow side. Interestingly, collagen deposition and matrix absorption throughout the base, middle, and tip of the BTHV leaflet increased progressively over time in iteration D.

In the field of bioresorbable material, there is always a dilemma resulting from two biological competing processes. One aspect is to maintain the mechanical properties responsible for a well-functioning valve for as long as possible; the other aspect is to allow for biodegradation of the material so that the restorative process and its growing mechanical strength can take over the loss of the mechanical properties of the original biodegradable structures. Therefore, tears may stem from a chronological mismatch between these two competing processes - neotissue build-up and implant bioabsorption. However, the occurrence of tears might be aggravated by some inherent properties of the sheep model, which is well known for its tendency to become calcified and by the peculiar frame design that might generate pinwheeling, leaflet redundancy, exaggerated leaflet coaptation, and premature tissue fatigue and alteration.

Pinwheeling has previously been described as one of the major mechanisms of bioprosthetic heart valve failure, causing early leaflet fatigue[29]. Pinwheeling is related to the valve design, device sizing and implantation. The leaflets must be designed to have sufficient length to close the valve without a coaptation gap or coaptation redundancy. Indeed, when the valve is oversized or underexpanded due to calcification, the redundant free edges of the leaflet must bend and plicate to accommodate the morphological anatomy of complete valve closure. It has been demonstrated that pinwheeling of valves can produce an asymmetric leaflet strain pattern[30], which may result in leaflet fatigue.

The stent post deflection in the current nitinol frame design may cause bending of the leaflet free edge and plication, and consequently increase the mechanical stress, potentially triggering SVD and calcification processes.

Nonetheless, iteration D was the most stable among all the iterations up to 12-month follow-up. This finding suggests that iteration D holds most promise towards providing a BTHV. Future studies will be carried out to increase mechanistic understanding of this striking observation.

Limitations

There are several limitations to be acknowledged. First, while reasonable efforts should be made to mimic the human situation, it should be realised that there will always be differences between human and animal models. Sheep have a very short aortic root, and therefore limited space for positioning the valve. In addition, the sheep aortic and mitral valves are very close to each other and reside in the same plane. These challenges might lead to an ill-positioned or too long aortic valve prosthesis, which may cause mitral valve damage because of abrasion against the aortic valve prosthesis. We could solve this by using a short design of the prosthesis and appropriate cushioning of parts that are at risk of causing abrasion. Another challenge is related to the absence of stenosis and calcification in our ovine model. In the present study, no attempt was made to create stenosis or regurgitation, or to alter the valve (e.g., inducing calcification) prior to its replacement. In other words, the leaflets were healthy in this ovine model. Thereby, there was the necessity to adopt the clipping mechanism of the leaflets for anchoring the metallic platform in these healthy aortic valves; the balloon-expandable technique would have easily ruptured the aortic annulus and the aortas of the sheep which have very thin and fragile aortic valve cusps compared to the human. Furthermore, anchoring would have been inadequate and insufficient due to the lack of a calcified landing zone. Therefore, in our analysis, the self-expanding Xeltis BTHV (transapical) with clipping of the leaflet was selected and used. Another alternative would have been a purely self-expanding valve (i.e., CoreValve type). At the time of the study design, no previous experience with this type of valve had been reported in the peer-reviewed literature. Since the position of our valve is based on feelers that sit on the native cusps, further cushioning of the tip of the feelers was required to avoid perforation of these thin native cusps by the feelers. Second, radiography was used to assess integrity of the leaflet polymer, which is not a standardised method; a discontinuity in the polymer looks like a hole in radiography while this could be an area that is still covered with tissue. For assessing the BTHV leaflets, a reasonable effort in developing and optimising the ovine model has been made. However, considering the usage of normal animals for the current experiments, the chronic performance of the BTHV could be different between a non-aortic stenosis recipient and an aortic stenosis recipient, suggesting that further investigations are needed for confirmation. Third, stent post deflection was defined and quantified based on the distance between two post tips on angiography. The 2D measurements may not fully represent the geometry of stent post deflection. In addition, biomechanical testing was not routinely performed in each valve/animal. Furthermore, stress analysis of valves was not implemented in the

study design and therefore further investigations are still needed to explore our observations in the preclinical study. Finally, this is a conceptional study comprising a small number of animals in each group with a focus on material selection. Therefore, we did not perform formal inter-group statistical analysis.

Conclusions

Several leaflet material iterations were compared for potential to demonstrate endogenous tissue restoration in an aortic valve *in vivo*. The most promising iteration near design freeze showed intact leaflets and acceptable haemodynamic performance at 12 months, illustrating the potential of the BTHV for systemic applications. Material optimisation was critical for achieving proof of feasibility. Further studies including stent frame optimisation will be critical towards achieving even more robust proof of concept.

Impact on daily practice

The present study reports, for the first time, a favourable haemodynamic performance up to 12 months of a BTHV in a high-pressure environment. Before deciding upon extensive and long-term evaluation of this cutting-edge technology that has the potential to change our clinical approach drastically, it was essential to eliminate the device configuration that would not work and to identify the best option before getting engaged in the second phase of animal evaluation. Biostable polymeric leaflets (Foldax technology; Foldax, Inc., Salt Lake City, UT, USA) are currently in clinical testing and the preclinical testing of a bioresorbable leaflet serving as a template for the restorative process is a new step forward. The main lesson of this study is that progress partially needs to rely on testing various iterations as part of a funnel-based selection process.

Conflict of interest statement

P.W. Serruys reports personal fees from SMT, Philips/Volcano, Xeltis, Novartis, and Meril Life. M. El-Kurdi, W. van den Bergh and M. Cox are employed by Xeltis. O. Soliman reports institutional research grants related to his work as the chairman of cardiovascular imaging core labs of several clinical trials and registries sponsored by industry, for which he receives no direct compensation. The other authors have no conflicts of interest to declare.

References

1. Mack MJ, Leon MB, Thourani VH, Makkar R, Kodali SK, Russo M, Kapadia SR, Malaisrie SC, Cohen DJ, Pibarot P, Leipsic J, Hahn RT, Blanke P, Williams MR, McCabe JM, Brown DL, Babaliaros V, Goldman S, Szeto WY, Genereux P, Pershad A, Pocock SJ, Alu MC, Webb JG, Smith CR; PARTNER 3 Investigators. Transcatheter Aortic-Valve Replacement with a Balloon-Expandable Valve in Low-Risk Patients. *N Engl J Med.* 2019;380:1695-705.

2. Popma JJ, Deeb GM, Yakubov SJ, Mumtaz M, Gada H, O'Hair D, Bajwa T, Heiser JC, Merhi W, Kleiman NS, Askew J, Sorajja P, Rovin J, Chetcuti SJ, Adams DH, Teirstein PS, Zorn GL 3rd, Forrest JK, Tchétché D, Resar J, Walton A, Piazza N, Ramlawi B, Robinson N, Petrossian G, Gleason TG, Oh JK, Boulware MJ, Qiao H, Mugglin AS, Reardon MJ; Evolut Low Risk Trial Investigators. Transcatheter Aortic-Valve Replacement with a Self-Expanding Valve in Low-Risk Patients. *N Engl J Med.* 2019;380:1706-15.

3. Rodriguez-Gabella T, Voisine P, Puri R, Pibarot P, Rodés-Cabau J. Aortic Bioprosthetic Valve Durability: Incidence, Mechanisms, Predictors, and Management of Surgical and Transcatheter Valve Degeneration. *J Am Coll Cardiol.* 2017;70:1013-28.

4. Serruys PW, Miyazaki Y, Katsikis A, Abdelghani M, Leon MB, Virmani R, Carrel T, Cox M, Onuma Y, Soliman OII. Restorative valve therapy by endogenous tissue restoration: tomorrow's world? Reflection on the EuroPCR 2017 session on endogenous tissue restoration. *EuroIntervention.* 2017;13:AA68-77.

5. De Visscher G, Blockx H, Meuris B, Van Oosterwyck H, Verbeken E, Herregods MC, Flameng W. Functional and biomechanical evaluation of a completely recellularized stentless pulmonary bioprosthesis in sheep. *J Thorac Cardiovasc Surg.* 2008;135:395-404.

6. De Visscher G, Lebacq A, Mesure L, Blockx H, Vranken I, Plusquin R, Meuris B, Herregods MC, Van Oosterwyck H, Flameng W. The remodeling of cardiovascular bioprostheses under influence of stem cell homing signal pathways. *Biomaterials.* 2010;31:20-8.

7. Syedain ZH, Haynie B, Johnson SL, Lahti M, Berry J, Carney JP, Li J, Hill RC, Hansen KC, Thrivikraman G, Bianco R, Tranquillo RT. Pediatric tri-tube valved conduits made from fibroblast-produced extracellular matrix evaluated over 52 weeks in growing lambs. *Sci Transl Med.* 2021;13:eabb7225.

8. Emmert MY, Schmitt BA, Loerakker S, Sanders B, Spriestersbach H, Fioretta ES, Bruder L, Brakmann K, Motta SE, Lintas V, Dijkman PE, Frese L, Berger F, Baaijens FPT, Hoerstrup SP. Computational modeling guides tissue-engineered heart valve design for long-term in vivo performance in a translational sheep model. *Sci Transl Med.* 2018;10:eaan4587.

9. Syedain Z, Reimer J, Schmidt J, Lahti M, Berry J, Bianco R, Tranquillo RT. 6-month aortic valve implantation of an off-the-shelf tissue-engineered valve in sheep. *Biomaterials.* 2015;73:175-84.

10. Poulis N, Zaytseva P, Gahwiler EKN, Motta SE, Fioretta ES, Cesarovic N, Falk V, Hoerstrup SP, Emmert MY. Tissue engineered heart valves for transcatheter aortic valve implantation: current state, challenges, and future developments. *Expert Rev Cardiovasc Ther.* 2020;18:681-96.

11. Uiterwijk M, Smits A, van Geemen D, van Klarenbosch B, Dekker S, Cramer MJ, van Rijswijk JW, Lurier EB, Di Luca A, Brugmans MCP, Mes T, Bosman AW, Aikawa E, Grundeman PF, Bouten CVC, Kluin J. In Situ Remodeling Overrules Bioinspired Scaffold Architecture of Supramolecular Elastomeric Tissue-Engineered Heart Valves. *JACC Basic Transl Sci.* 2020;5:1187-206.

12. Brugmans M, Serrero A, Cox M, Svanidze O, Schoen FJ. Morphology and mechanisms of a novel absorbable polymeric conduit in the pulmonary circulation of sheep. *Cardiovasc Pathol.* 2019;38:31-8.

13. Bennink G, Torii S, Brugmans M, Cox M, Svanidze O, Ladich E, Carrel T, Virmani R. A novel restorative pulmonary valved conduit in a chronic sheep model: Mid-term hemodynamic function and histologic assessment. *J Thorac Cardiovasc Surg.* 2018;155:2591-601.

14. Soliman OI, Miyazaki Y, Abdelghani M, Brugmans M, Witsenburg M, Onuma Y, Cox M, Serruys PW. Midterm performance of a novel restorative pulmonary valved conduit: preclinical results. *EuroIntervention.* 2017;13:e1418-27.

15. Kluin J, Talacua H, Smits AI, Emmert MY, Brugmans MC, Fioretta ES, Dijkman PE, Söntjens SH, Duijvelshoff R, Dekker S, Janssen-van den Broek MW, Lintas V, Vink A, Hoerstrup SP, Janssen HM, Dankers PY, Baaijens FP, Bouten CV. In situ heart valve tissue engineering using a bioresorbable elastomeric implant - From material design to 12 months follow-up in sheep. *Biomaterials.* 2017;125:101-17.

16. Morales DL, Herrington C, Bacha EA, Morell VO, Prodan Z, Mroczek T, Sivalingam S, Cox M, Bennink G, Asch FM. A Novel Restorative Pulmonary Valve Conduit: Early Outcomes of Two Clinical Trials. *Front Cardiovasc Med.* 2020;7:583360.

17. Bockeria LA, Svanidze O, Kim A, Shatalov K, Makarenko V, Cox M, Carrel T. Total cavopulmonary connection with a new bioabsorbable vascular graft: First clinical experience. *J Thorac Cardiovasc Surg.* 2017;153:1542-50.

18. Miyazaki Y, Soliman OII, Abdelghani M, Katsikis A, Naz C, Lopes S, Warnack B, Cox M, Onuma Y, Serruys PW. Acute performance of a novel restorative transcatheter aortic valve: preclinical results. *EuroIntervention.* 2017;13:e1410-7.

19. Webber MJ, Appel EA, Meijer EW, Langer R. Supramolecular biomaterials. *Nat Mater.* 2016;15:13-26.

20. Sijbesma RP, Beijer FH, Brunsveld L, Folmer BJ, Hirschberg JH, Lange RF, Lowe JK, Meijer EW. Reversible polymers formed from self-complementary monomers using quadruple hydrogen bonding. *Science.* 1997;278:1601-4.

21. Modolo R, Chang CC, Onuma Y, Schultz C, Tateishi H, Abdelghani M, Miyazaki Y, Aben JP, Rutten MCM, Pighi M, El Bouziani A, van Mourik M, Lemos PA, Wykrzykowska JJ, Brito FS Jr, Sahyoun C, Piazza N, Eltchaninoff H, Soliman O, Abdel-Wahab M, Van Mieghem NM, de Winter RJ, Serruys PW. Quantitative aortography assessment of aortic regurgitation. *EuroIntervention.* 2020;16:e738-56.

22. Kawashima H, Wang R, Mylotte D, Jagielak D, De Marco F, Ielasi A, Onuma Y, den Heijer P, Terkelsen CJ, Wijns W, Serruys PW, Soliman O. Quantitative Angiographic Assessment of Aortic Regurgitation after Transcatheter Aortic Valve Implantation among Three Balloon-Expandable Valves. *Glob Heart.* 2021;16:20.

23. Zoghbi WA, Asch FM, Bruce C, Gillam LD, Grayburn PA, Hahn RT, Inglessis I, Islam AM, Lerakis S, Little SH, Siegel RJ, Skubas N, Slesnick TC, Stewart WJ, Thavendiranathan P, Weissman NJ, Yasukochi S, Zimmerman KG. Guidelines for the Evaluation of Valvular Regurgitation After Percutaneous Valve Repair or Replacement: A Report from the American Society of Echocardiography Developed in Collaboration with the Society for Cardiovascular Angiography and Interventions, Japanese Society of Echocardiography, and Society for Cardiovascular Magnetic Resonance. *J Am Soc Echocardiogr.* 2019;32:431-75.

24. Kappetein AP, Head SJ, Généreux P, Piazza N, van Mieghem NM, Blackstone EH, Brott TG, Cohen DJ, Cutlip DE, van Es GA, Hahn RT, Kirtane AJ, Krucoff MW, Kodali S, Mack MJ, Mehran R, Rodés-Cabau J, Vranckx P, Webb JG, Windecker S, Serruys PW, Leon MB. Updated standardized endpoint definitions for transcatheter aortic valve implantation: the Valve Academic Research Consortium-2 consensus document. *Eur Heart J.* 2012;33:2403-18.

25. Jamieson WR, Ling H, Burr LH, Fradet GJ, Miyagishima RT, Janusz MT, Lichtenstein SV. Carpentier-Edwards supraannular porcine bioprosthesis evaluation over 15 years. *Ann Thorac Surg.* 1998;66:S49-52.

26. Schoen FJ, Levy RJ. Calcification of tissue heart valve substitutes: progress toward understanding and prevention. *Ann Thorac Surg.* 2005;79:1072-80.

27. Siddiqui RF, Abraham JR, Butany J. Bioprosthetic heart valves: modes of failure. *Histopathology.* 2009;55:135-44.

28. Bourguignon T, Bouquiaux-Stablo AL, Candolfi P, Mirza A, Loardi C, May MA, El-Khoury R, Marchand M, Aupart M. Very long-term outcomes of the Carpentier-Edwards Perimount valve in aortic position. *Ann Thorac Surg.* 2015;99:831-7.

29. Schoen FJ, Schulman LJ, Cohn LH. Quantitative anatomic analysis of "stent creep" of explanted Hancock standard porcine bioprostheses used for cardiac valve replacement. *Am J Cardiol.* 1985;56:110-4.

30. Gunning PS, Saikrishnan N, Yoganathan AP, McNamara LM. Total ellipse of the heart valve: the impact of eccentric stent distortion on the regional dynamic deformation of pericardial tissue leaflets of a transcatheter aortic valve replacement. *J R Soc Interface.* 2015;12:20150737.

Supplementary data

Supplementary Appendix 1. Extended methods section.

Supplementary Appendix 2. Extended results section.

Supplementary Table 1. Quantification of diastolic stent post inward deflection on angiography.

Supplementary Table 2. Individual findings of aortography and echocardiography among the five design iterations.

Supplementary Table 3. Different types of AR severity on echocardiography among the five design iterations.

Supplementary Figure 1. *In vitro* testing – animal fixture versus human fixture.

Supplementary Figure 2. Classification of the leaflet morphology on radiographic images.

Supplementary Figure 3. Transition of median VD-AR at implantation (acute phase) and before scheduled euthanasia (chronic phase) among the five iterations.

Supplementary Figure 4. Results of each pathological score in the iterations A, B, B', and C.

Supplementary Figure 5. Leaflet integrity assessment on radiographic images.

The supplementary data are published online at: https://eurointervention.pcronline.com/doi/10.4244/EIJ-D-21-00386

Supplementary data

Supplementary Appendix 1. Extended methods section

TAVI procedure

All procedures were performed under general anaesthesia. The BTHV were implanted using a transapical approach under the guidance of echocardiography, fluoroscopy, and aortography. A pigtail catheter was introduced transfemorally and placed in the native aortic valve cusp as reference for positioning. The valve was delivered transapically using fluoroscopy guidance. The distal end of the valve was deployed first; afterwards, the delivery system was pulled gently to anchor the three device arms into the sinuses of Valsalva, prior to full deployment and release of the device. Predilatation or post-dilatation was not performed.

Quantification of aortic valve stent post deflection

Aortic valve stent post deflection was quantified in both acute and chronic phases by an independent academic core laboratory (CORRIB Research Centre for Advanced Imaging and Core Lab, Galway, Ireland) by experienced analysts who were blinded to other imaging data and anatomo-pathological results. The distance (D) between two post tips on angiography was measured at the systolic and diastolic phase, using CAAS 5.11 Workstation (Pie Medical Imaging, Maastricht, the Netherlands). Absolute stent post inward deflection referred to the change of distance between post tips in one cardiac cycle (i.e., absolute stent post inward deflection = distance in systolic phase [*Ds*] minus distance in diastolic phase [*Dd]*). Relative stent post inward deflection (%) was calculated using the following equation: $\frac{\mathrm{Ds}-\mathrm{Dd}}{\mathrm{Ds}}$ x 100

Details of calculations of the leaflet thickness score, thrombus score, collagen deposition score, matrix absorption score, and inflammation score

Leaflet thickness score, 0 (no neointima) to 4

Leaflet thickness score as follows: 1, less than/or equal to leaflet thickness; 2, greater than leaflet thickness, but less than 2x the thickness; 3, greater than 2x leaflet thickness, but less than 4x the thickness; 4, greater than 4x the thickness.

Thrombus score, 0 (no thrombus) to 4

Thrombus score as follows: 1, minimal fibrin/thrombus deposition involving <10% of the leaflet surface; 2, mild fibrin/thrombus deposition involving 10%-25% of the leaflet surface; 3, moderate fibrin/thrombus deposition involving >25%-50% of the leaflet surface; 4, severe fibrin/thrombus deposition involving >50% of the leaflet surface.

Collagen deposition score, 1 to 5

Collagen deposition score as follows: 1, <10% leaflet matrix; 2, 10-<25% leaflet matrix; 3, 25%-<50% leaflet matrix; 4, 50%-<75% leaflet matrix; 5, >75% leaflet matrix.

Matrix absorption score, 1 to 5

Matrix absorption score as follows: 1, <10% leaflet matrix; 2, 10-<25% leaflet matrix; 3, 25%-<50% leaflet matrix; 4, 50%-<75% leaflet matrix; 5, >75% leaflet matrix.

Inflammation score, 0 (no inflammation) to 4
Inflammation score as follows: 1, rare inflammatory cell infiltration; 2, mild infiltrate and is not the predominant component of the associated tissue; 3, infiltrates up to ½ of the leaflet; 4, infiltrates > ½ of the leaflet.

In vitro biomechanical testing and pinwheeling index
To acquire the image series of the valve opening and closure in vitro, a high-speed camera set-up was used. Pinwheeling index was quantified using en face data by tracing the length of the leaflet free edges and comparing them to their unconstrained and ideal iterations. The pinwheeling index is computed by the following equation:

$$\text{Pinwheeling index (\%)} = \frac{\text{Lactual} - \text{Lideal}}{\text{Lideal}} \text{ x } 100$$

Supplementary Appendix 2. Extended results section
Aortic valve stent post deflection and pinwheeling
Quantification of diastolic stent post inward deflections on aortography following TAVR (acute phase) is presented in **Supplementary Table 1**. On average, valve stent post inward deflection was 12.7%. The potential adverse effect of post inward deflection was assessed in an in vitro pulse duplicator using fixtures of different sizes **(Supplementary Figure 1)**.

Gross anatomo-pathological inspection of leaflet
Leaflet and scaffold thickness measurements
In iteration A, the base tissue increased between 6 and 12 months on the outflow side (304.8 µm to 857.6 µm). In iteration B, the base tissue decreased between 6 and 12 months on the inflow side (649.0 µm to 287.5 µm). In iteration B', the base tissue increased between 6 and 12 months on the outflow side (215.7 µm to 418.3 µm). In iteration C, the base tissue increased between 6 and 12 months on the outflow side (267.4 µm to 506.6 µm). In iteration D, the base tissue increased between 6 and 12 months on the outflow side (212.4 µm to 420.0 µm), and the middle tissue also increased (374.4 µm to 471.0 µm).

Supplementary Table 1. Quantification of diastolic stent post inward deflection on angiography.

	After implantation (acute phase)			
Iteration	Ds (mm)	Dd (mm)	Absolute inward deflection (mm)	Relative inward deflection (%)
A	19.7±2.8	17.1±2.2	2.6±1.0	13
B	17.9±2.9	16.0±2.8	1.9±0.3	11
B’	21.3±1.7	18.5±2.0	2.7±0.6	13
C	18.9±2.3	16.4±1.8	2.5±0.8	13
D	18.1±0.8	15.6±0.8	2.5±0.7	14

Absolute inward deflection = Ds-Dd.

Relative inward deflection = Ds-Dd/Ds.

Dd: distance between two stent post tips on angiography at diastolic phase; Ds: distance between two stent post tips on angiography at systolic phase

Supplementary Table 2. Individual findings of aortography and echocardiography among the five design iterations.

		Aortography (aortic regurgitation)				Echocardiography (haemodynamic performance and aortic regurgitation)															
		*VD-AR, %				AR severity grade				Peak PG, mmHg				**Mean PG, mmHg				***EOA, cm²			
No	Iteration	Implantation	3 months	6 months	12 months	7 days	3 months	6 months	12 months	7 days	3 months	6 months	12 months	7 days	3 months	6 months	12 months	7 days	3 months	6 months	12 months
1	A	5	NA	25	NA	1	1	0	NA	5	16	11	NA	2	6	5	NA	2.3	1.3	1.5	NA
2	A	0	NA	4	NA	0	1	3	NA	8	7	18	NA	4	3	8	NA	2.2	1.7	1.8	NA
3	A	NA	NA	NA	NA	0	2	NA	NA	8	4	NA	NA	5	2	NA	NA	2.0	2.3	NA	NA
4	A	2	1	NA	NA	1	1	NA	NA	6	17	NA	NA	3	7	NA	NA	2.8	1.2	NA	NA
5	A	1	1	NA	NA	1	1	NA	NA	9	18	NA	NA	5	10	NA	NA	2.1	1.2	NA	NA
6	A	16	NA	NA	1	2	1	1	1	17	22	19	17	7	8	9	8	1.7	1.1	0.9	0.5
7	A	4	NA	NA	15	1	1	1	2	13	18	17	18	6	7	7	12	1.5	1.5	1.4	1.0
8	A	NA	NA	NA	NA	1	2	NA	NA	12	9	NA	NA	5	5	NA	NA	1.5	1.8	NA	NA
9	B	0	NA	10	NA	1	1	2	NA	9	4	3	NA	4	2	2	NA	4.0	2.5	2.0	NA
10	B	9	NA	9	NA	1	1	2	NA	10	9	17	NA	5	4	8	NA	2.3	2.3	1.8	NA
11	B	19	NA	2	NA	1	1	1	NA	10	4	7	NA	4	2	3	NA	2.6	2.9	2.6	NA
12	B	11	14	NA	NA	2	2	NA	NA	19	7	NA	NA	6	4	NA	NA	1.8	1.9	NA	NA
13	B	16	4	NA	NA	1	2	NA	NA	8	7	NA	NA	3	4	NA	NA	2.2	2.6	NA	NA
14	B	7	NA	NA	54	1	1	1	4	14	8	13	31	7	5	7	20	2.1	1.7	1.5	0.7
15	B	5	NA	NA	88	2	1	1	4	12	10	16	34	5	4	6	18	1.6	2.0	1.2	1.3
16	B	9	NA	NA	55	2	2	2	4	10	9	12	30	5	4	6	19	1.8	2.0	1.4	1.2
17	B'	NA	NA	18	NA	1	1	0	NA	10	14	19	NA	5	7	9	NA	1.4	1.5	1.2	NA
18	B'	NA	NA	2	NA	1	2	2	NA	7	17	22	NA	3	10	16	NA	2.1	1.1	0.7	NA
19	B'	14	NA	53	NA	1	2	2	NA	12	7	17	NA	6	4	4	NA	2.6	2.4	2.5	NA
20	B'	6	NA	NA	18	1	2	1	2	11	12	16	20	4	4	8	10	2.7	1.9	1.9	0.6
21	B'	6	NA	NA	37	0	2	2	4	5	6	12	13	3	3	5	7	2.7	2.0	2.5	1.4
22	B'	1	NA	NA	18	1	1	1	2	10	11	13	13	4	5	7	7	2.4	1.9	2.0	2.6
23	C	4	NA	1	NA	2	2	0	NA	9	17	11	NA	3	2	4	NA	2.4	2.5	1.5	NA
24	C	4	NA	49	NA	1	1	2	NA	7	7	13	NA	2	3	8	NA	1.6	2.2	2.8	NA
25	C	6	NA	80	NA	1	1	1	NA	8	9	20	NA	4	5	9	NA	1.6	1.8	1.3	NA
26	C	0	NA	NA	12	1	2	3	4	9	11	22	45	4	5	13	30	2.3	2.1	2.3	2.2
27	C	2	NA	NA	58	2	1	2	4	9	4	19	41	5	2	8	26	2.2	2.7	3.4	1.0
28	C	6	9	NA	NA	1	3	NA	NA	9	16	NA	NA	5	7	NA	NA	2.1	2.9	NA	NA
29	C	NA	NA	NA	NA	1	1	NA	NA	7	7	NA	NA	3	3	NA	NA	2.1	1.8	NA	NA
30	C	38	NA	NA	46	3	1	2	3	7	7	9	45	4	3	4	25	2.6	1.5	1.7	1.4
31	D	1	NA	17	NA	1	1	2	NA	15	7	18	NA	6	3	11	NA	1.3	1.5	1.3	NA
32	D	1	NA	3	NA	2	1	1	NA	18	11	18	NA	8	6	9	NA	1.5	1.4	1.3	NA
33	D	3	NA	35	NA	1	1	2	NA	5	17	15	NA	4	9	7	NA	1.7	1.4	2.1	NA
34	D	1	3	NA	NA	1	2	NA	NA	11	20	NA	NA	5	11	NA	NA	1.4	1.3	NA	NA
35	D	7	2	NA	NA	1	2	NA	NA	11	26	NA	NA	5	13	NA	NA	2.1	1.0	NA	NA
36	D	3	4	NA	NA	1	0	NA	NA	11	13	NA	NA	5	6	NA	NA	1.7	1.8	NA	NA
37	D	2	NA	NA	1	1	1	1	1	17	13	21	21	7	7	12	13	1.3	1.7	1.1	0.5
38	D	3	NA	NA	9	1	0	0	1	11	17	15	13	4	6	6	7	1.7	2.6	1.4	1.3
39	D	6	NA	NA	19	1	2	2	2	21	5	27	22	10	2	9	14	1.2	3.0	1.8	1.2

Aortography was performed according to a pre-specified protocol immediately after TAVI [18] and before scheduled euthanasia. In the present study, VD-AR before euthanasia was analysable in 36 animals. The red letters in the Table represent abnormal values according to the following definition:

*More than 17% of VD-AR is considered as significant aortic regurgitation on aortography in clinic [21,22]. The same threshold has been applied here, although no reference framework exists on translation from ovine to human situation.

**Mean PG ≥20 mmHg is considered as abnormal [24].

***EOA ≤0.9 cm^2 is considered as abnormal [24].

AR: aortic regurgitation; EOA: effective orifice area; NA: not applicable/available; PG: pressure gradient; VD-AR: videodensitometric aortic regurgitation

Supplementary Table 3. Different types of AR severity on echocardiography among the five design iterations.

		Echocardiography (haemodynamic performance and aortic regurgitation)															
		AR severity grade (overall)				AR severity (transvalvular)				AR severity (commissural)				AR severity (paravalvular)			
No	Iteration	7 days	3 months	6 months	12 months	7 days	3 months	6 months	12 months	7 days	3 months	6 months	12 months	7 days	3 months	6 months	12 months
1	A	1	1	0	NA	1	0	0	NA	1	1	0	NA	0	0	0	NA
2	A	0	1	3	NA	0	0	3	NA	0	1	0	NA	0	0	0	NA
3	A	0	2	NA	NA	0	1	NA	NA	0	0	NA	NA	0	2	NA	NA
4	A	1	1	NA	NA	0	0	NA	NA	1	1	NA	NA	1	0	NA	NA
5	A	1	1	NA	NA	0	1	NA	NA	1	1	NA	NA	1	0	NA	NA
6	A	2	1	1	1	0	1	1	1	2	1	0	0	0	0	0	0
7	A	1	1	1	2	0	0	1	0	1	1	1	2	0	0	0	0
8	A	1	2	NA	NA	0	1	NA	NA	1	2	NA	NA	0	0	NA	NA
9	B	1	1	2	NA	1	1	2	NA	0	1	0	NA	0	0	0	NA
10	B	1	1	2	NA	1	0	2	NA	0	1	0	NA	0	0	0	NA
11	B	1	1	1	NA	0	0	0	NA	1	1	1	NA	1	0	0	NA
12	B	2	2	NA	NA	0	2	NA	NA	2	1	NA	NA	0	1	NA	NA
13	B	1	2	NA	NA	1	1	NA	NA	1	0	NA	NA	0	0	NA	NA
14	B	1	1	1	4	1	1	1	4	0	1	0	4	0	1	1	0
15	B	2	1	1	4	0	0	1	4	2	1	1	4	0	0	0	0
16	B	2	2	2	4	2	1	1	4	1	1	1	4	0	0	2	2
17	B'	1	1	0	NA	0	0	0	NA	1	1	1	NA	0	0	0	NA
18	B'	1	2	2	NA	0	2	2	NA	1	2	2	NA	0	1	0	NA
19	B'	1	2	2	NA	1	0	2	NA	0	0	1	NA	0	2	0	NA
20	B'	1	2	1	2	0	0	0	1	0	1	1	1	1	2	1	2
21	B'	0	2	2	4	0	0	0	4	0	0	1	4	0	2	2	0
22	B'	1	1	1	2	0	1	1	2	1	0	0	2	1	0	0	0
23	C	2	2	0	NA	2	0	0	NA	0	1	0	NA	0	2	0	NA
24	C	1	1	2	NA	1	1	2	NA	0	1	2	NA	0	0	0	NA
25	C	1	1	1	NA	0	0	1	NA	1	1	1	NA	0	1	0	NA
26	C	1	2	3	4	0	2	3	4	1	2	3	4	0	2	0	0
27	C	2	1	2	4	2	0	2	4	1	1	2	4	1	1	0	0
28	C	1	3	NA	NA	1	0	NA	NA	1	3	NA	NA	0	2	NA	NA
29	C	1	1	NA	NA	0	0	NA	NA	1	1	NA	NA	0	0	NA	NA
30	C	3	1	2	3	3	1	0	3	1	1	2	3	1	0	0	0
31	D	1	1	2	NA	0	1	1	NA	1	0	2	NA	0	0	1	NA
32	D	2	1	1	NA	1	0	1	NA	2	1	0	NA	0	0	0	NA
33	D	1	1	2	NA	0	0	2	NA	1	0	2	NA	1	0	0	NA
34	D	1	2	NA	NA	0	2	NA	NA	1	1	NA	NA	0	0	NA	NA
35	D	1	2	NA	NA	0	0	NA	NA	1	1	NA	NA	1	2	NA	NA
36	D	1	0	NA	NA	1	0	NA	NA	1	0	NA	NA	0	0	NA	NA
37	D	1	1	1	1	0	1	0	1	1	0	1	0	0	0	0	0
38	D	1	0	0	1	0	0	0	1	1	0	0	0	0	0	0	0
39	D	1	2	2	2	0	2	2	2	1	0	2	0	0	0	1	0

AR: aortic regurgitation; NA: not applicable/available

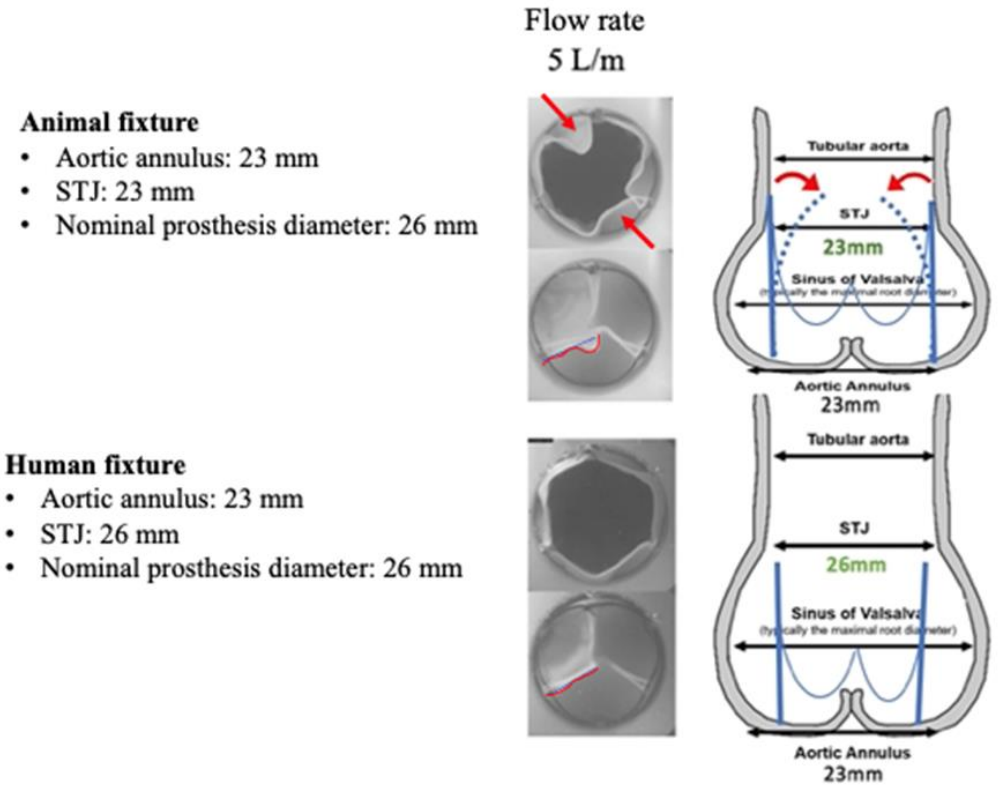

Supplementary Figure 1. In vitro testing - animal fixture versus human fixture.

Top panel: animal fixture (aortic annulus=23 mm, STJ=23 mm, nominal prosthesis diameter=26 mm) showed excessive local bending of leaflets (pinwheeling, red arrow) with immobile leaflets at flow rate of 5 L/minute. Lower panel: pinwheeling improved in the human fixture (aortic annulus=23 mm, STJ=26 mm, nominal prosthesis diameter=26 mm). $L_{actutal}$ (red line); L_{ideal} (blue line). STJ: sinotubular junction

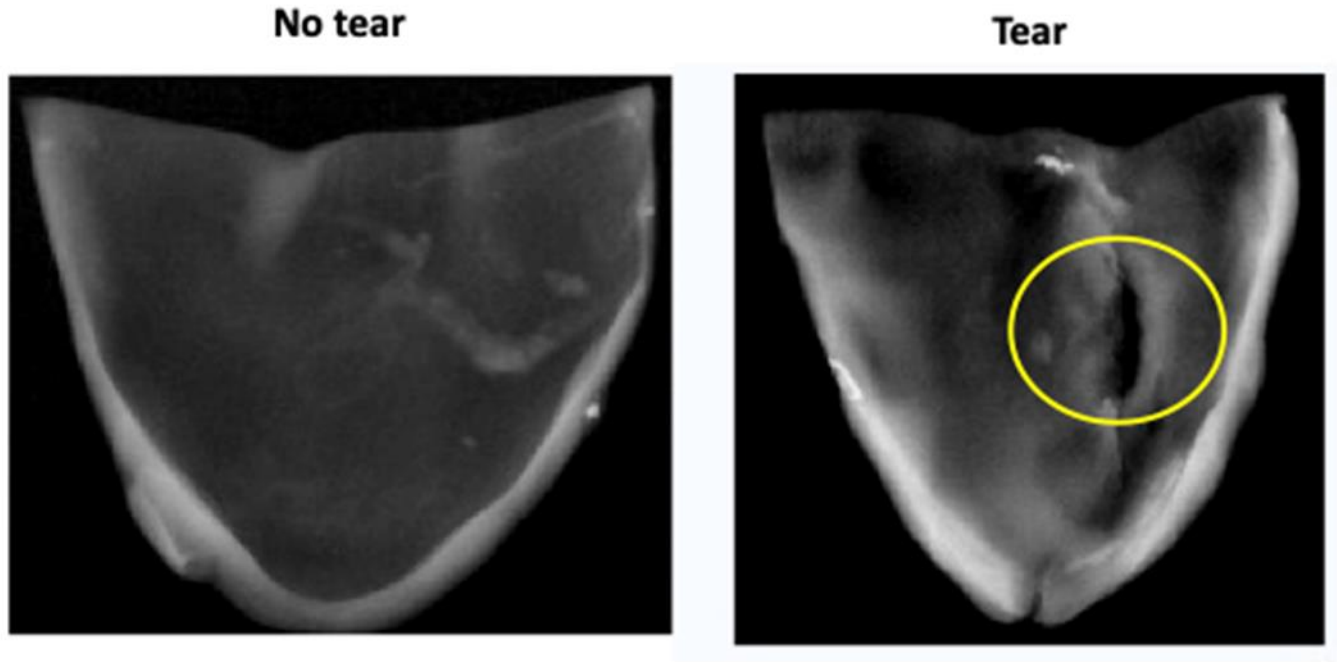

Supplementary Figure 2. Classification of the leaflet morphology on radiographic images.

Valve pathology classification based on radiographic images. Leaflet gross pathology was classified into two categories (no tear, tear) by visual inspection and corroborated on radiographic images. The yellow circle presents “tear".

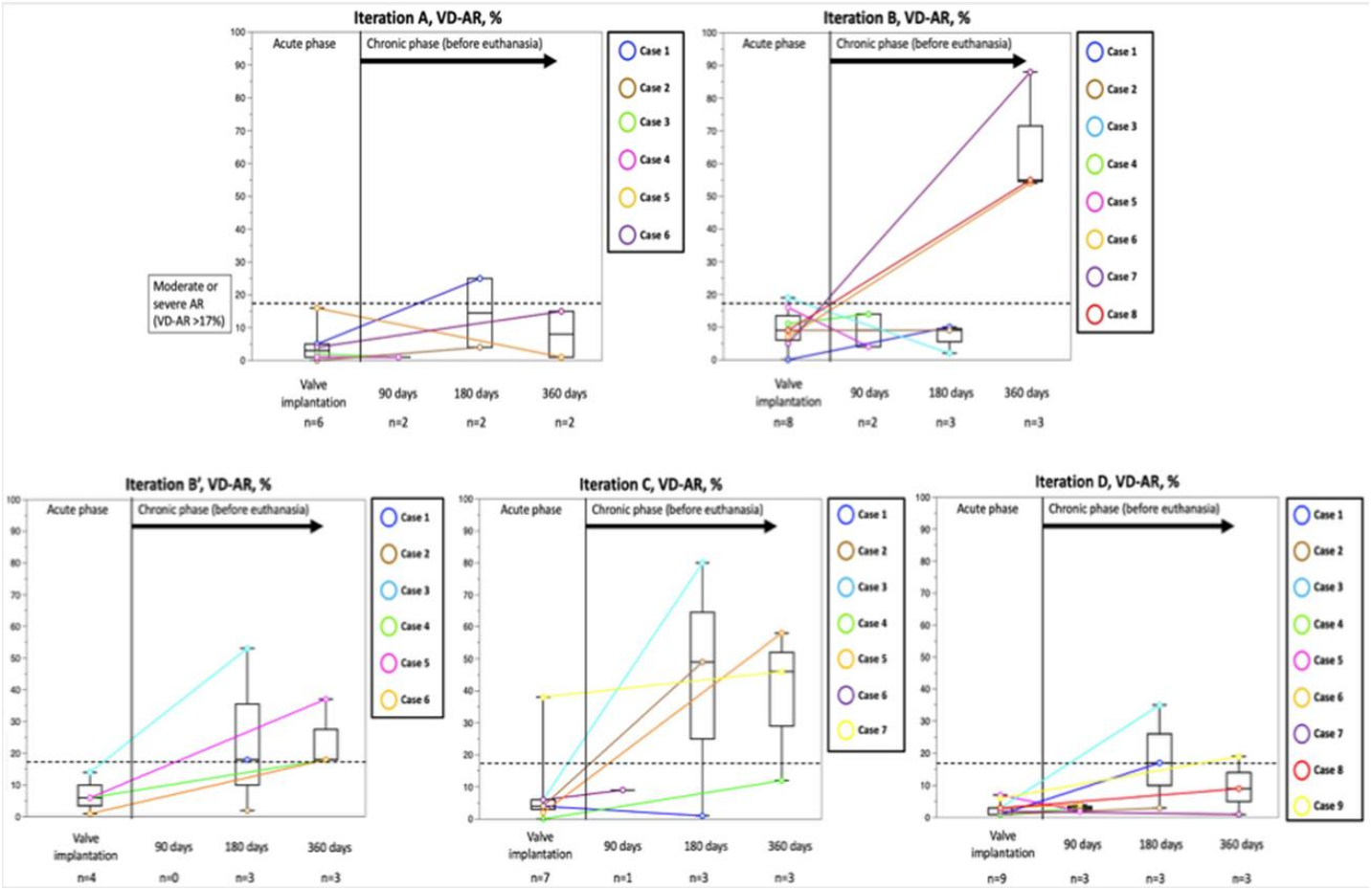

Supplementary Figure 3. Transition of median VD-AR at implantation (acute phase) and before scheduled euthanasia (chronic phase) among the five iterations.

The area above 17% of VD-AR, clinically used to indicate moderate or severe aortic regurgitation. Box-whisker plot of VD-AR of each sheep at implantation (acute phase), 90 days, 180 days, and 360 days (chronic phase). The upper and lower boundaries of the box represent the 75th and 25th percentiles, respectively. Whiskers above and below the box indicate the 90th and 10th percentiles, respectively. The bold line within the box marks the median. VD-AR: videodensitometric aortic regurgitation

4A

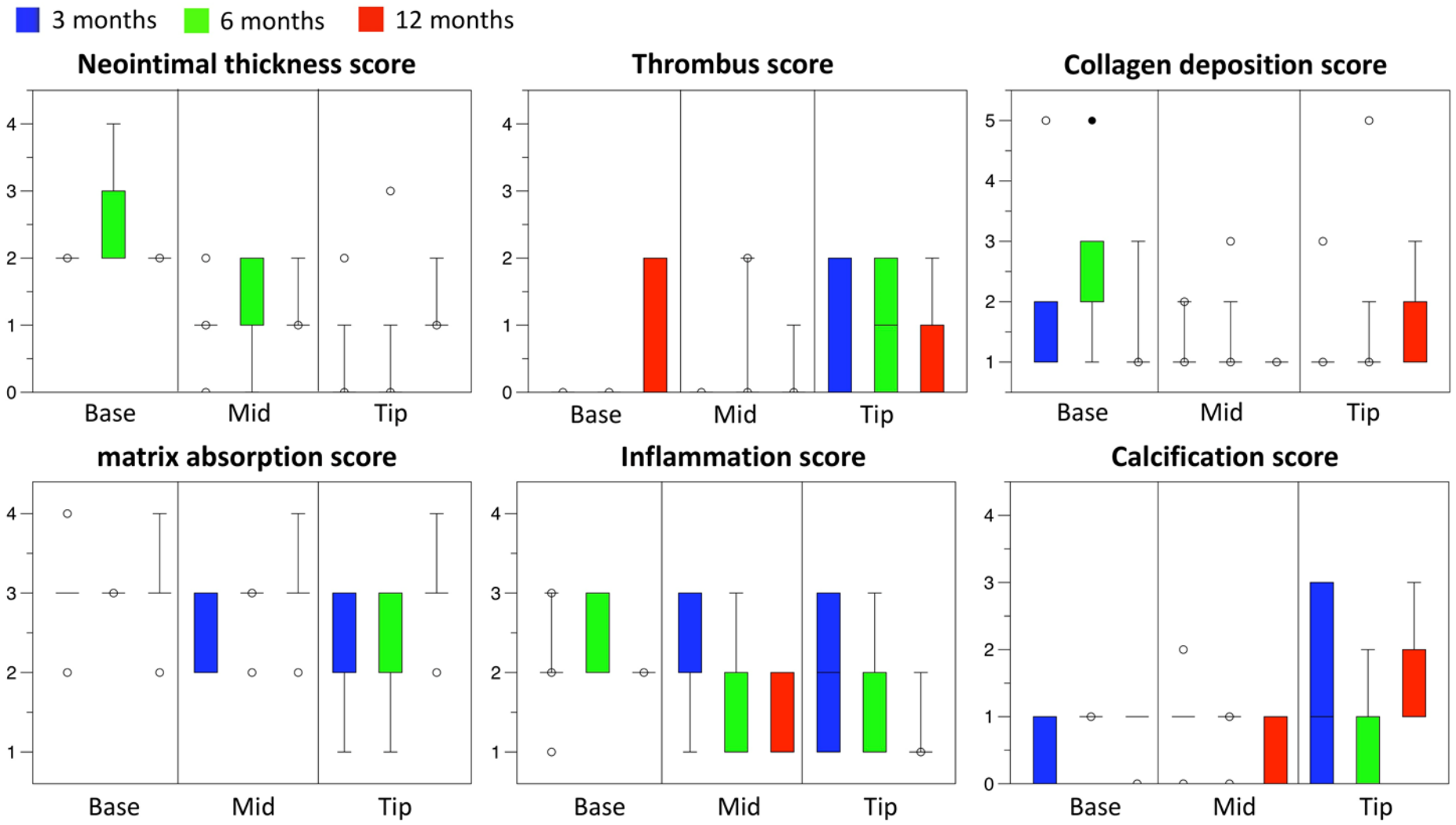
3 months
6 months
12 months
Neointimal thickness score
Thrombus score
Collagen deposition score
matrix absorption score
Inflammation score
Calcification score
Base
Mid
Tip

4B

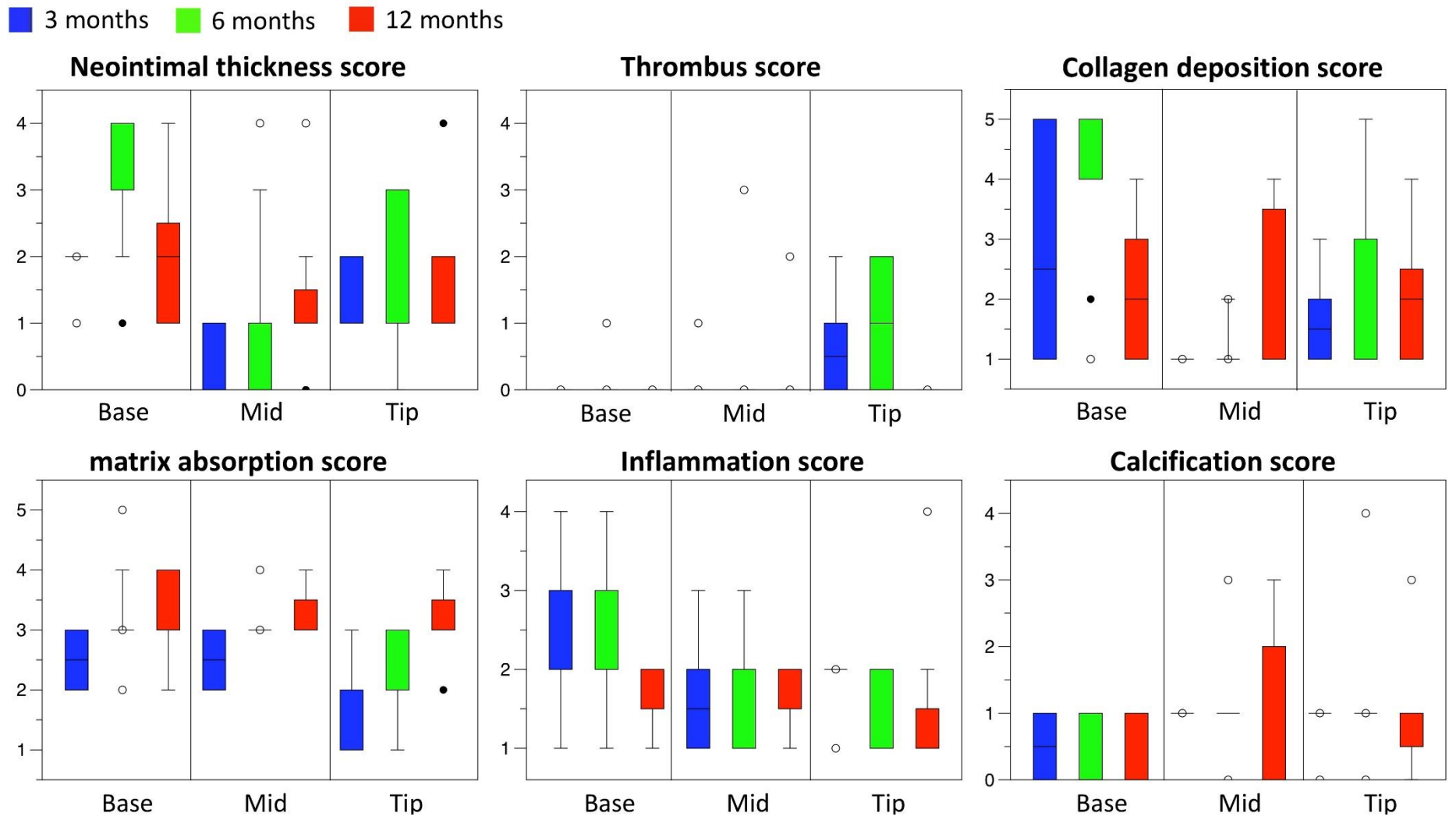
3 months
6 months
12 months
Neointimal thickness score
Thrombus score
Collagen deposition score
matrix absorption score
Inflammation score
Calcification score
Base
Mid
Tip

4B’

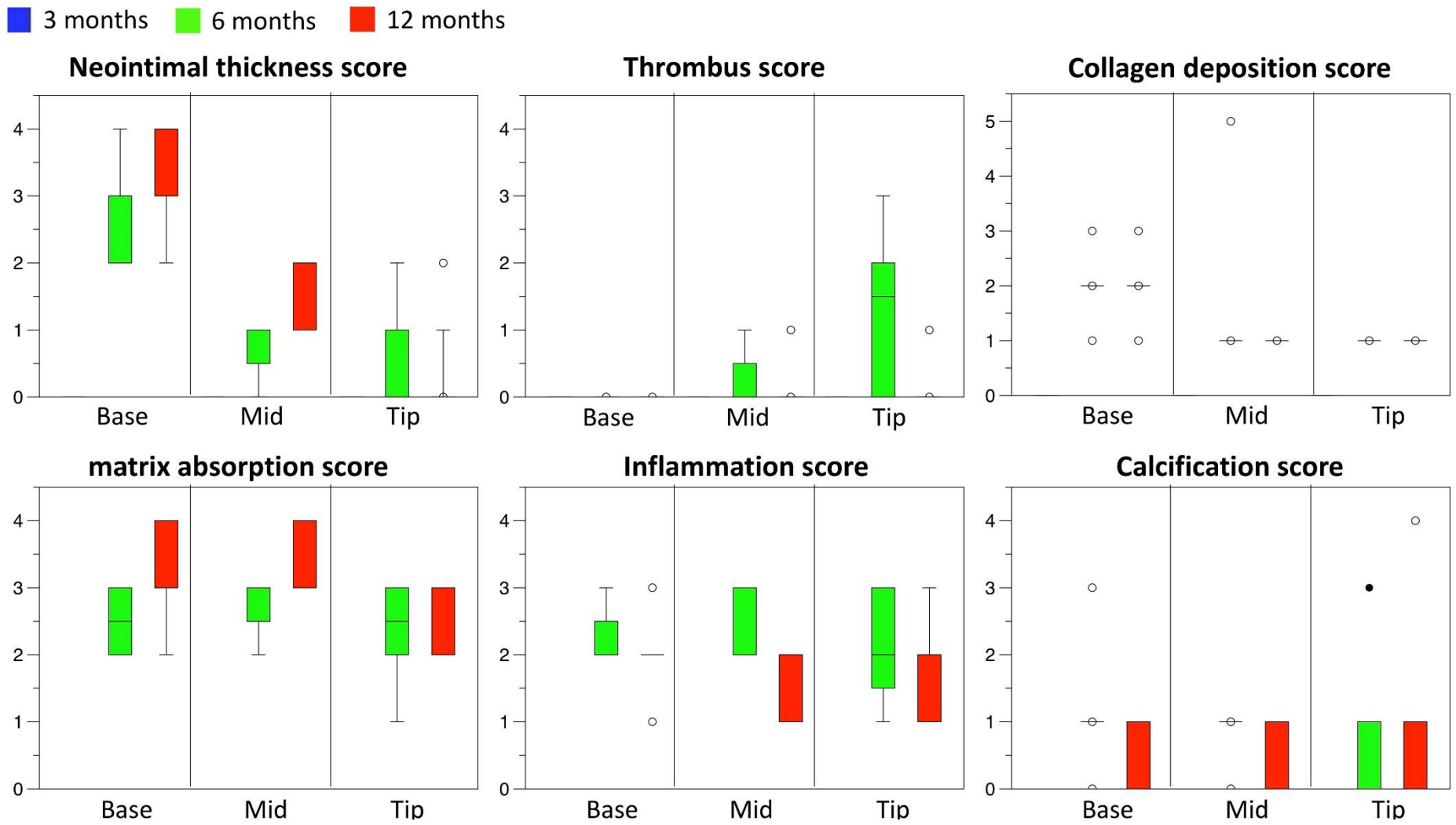
3 months
6 months
12 months
Neointimal thickness score
Thrombus score
Collagen deposition score
matrix absorption score
Inflammation score
Calcification score
Base
Mid
Tip

4C

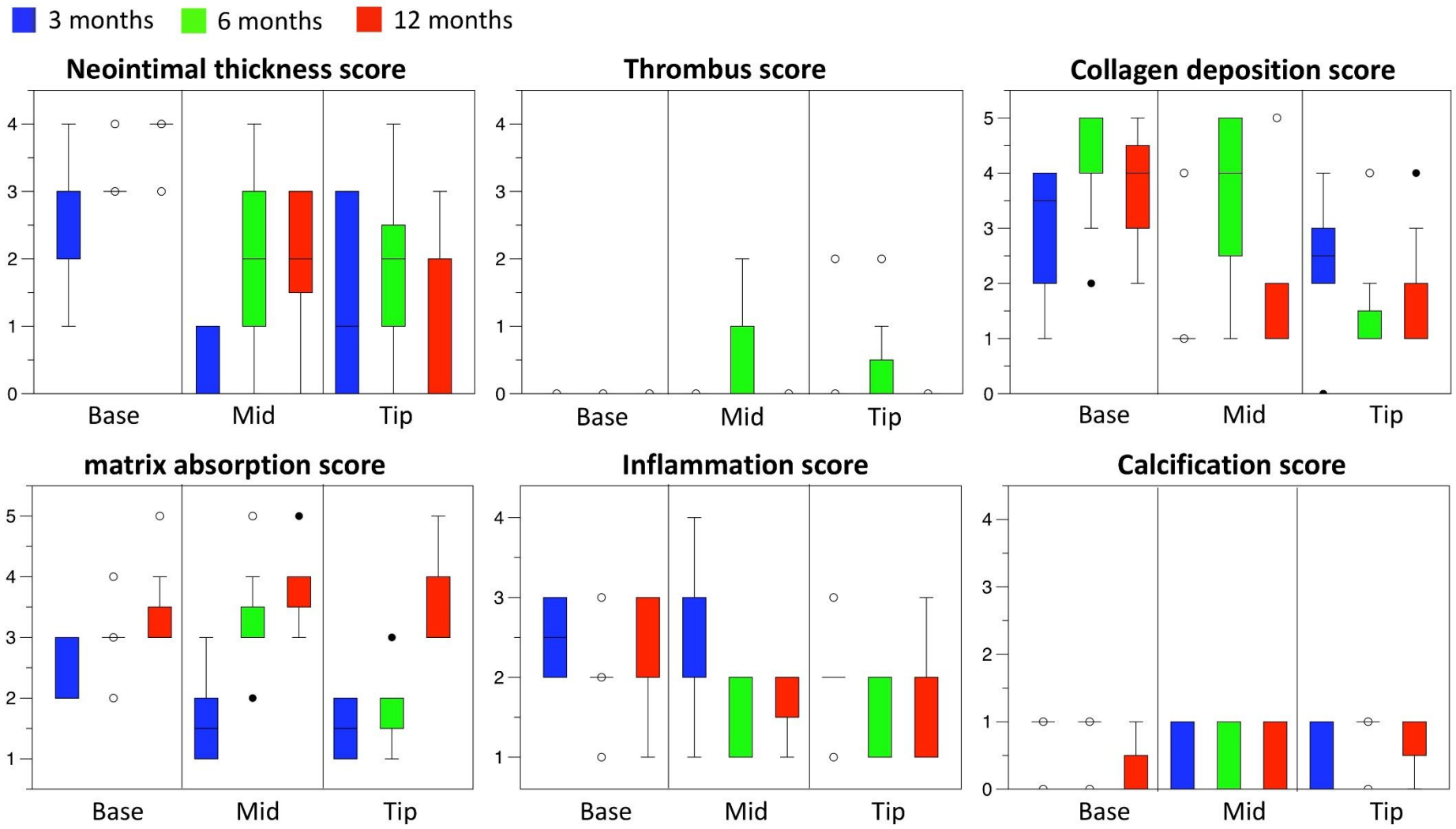
3 months
6 months
12 months
Neointimal thickness score
Thrombus score
Collagen deposition score
matrix absorption score
Inflammation score
Calcification score
Base
Mid
Tip

Supplementary Figure 4. Results of each pathological score in iterations A, B, B', and C.
Box-whisker plots of the neointimal thickness, thrombus, collagen deposition, matrix absorption, inflammation, and calcification scores at the base, middle, and tip of iterations A, B, B', and C at 3-, 6-, and 12-month follow-up are presented. The upper and lower boundaries of the box represent the 75th and 25th percentiles, respectively. Whiskers above and below the box indicate the maximum and minimum values, respectively. The line within the box marks the median. Outliers are drawn as filled in circles. An outlier is a value that is larger than 1.5 times the IQR from the median. IQR is the difference between the first and third quartiles. The whiskers are only drawn to the smallest/largest non-outlier. Extreme outliers that are three times the IQR are drawn as open circles.

IQR: interquartile range

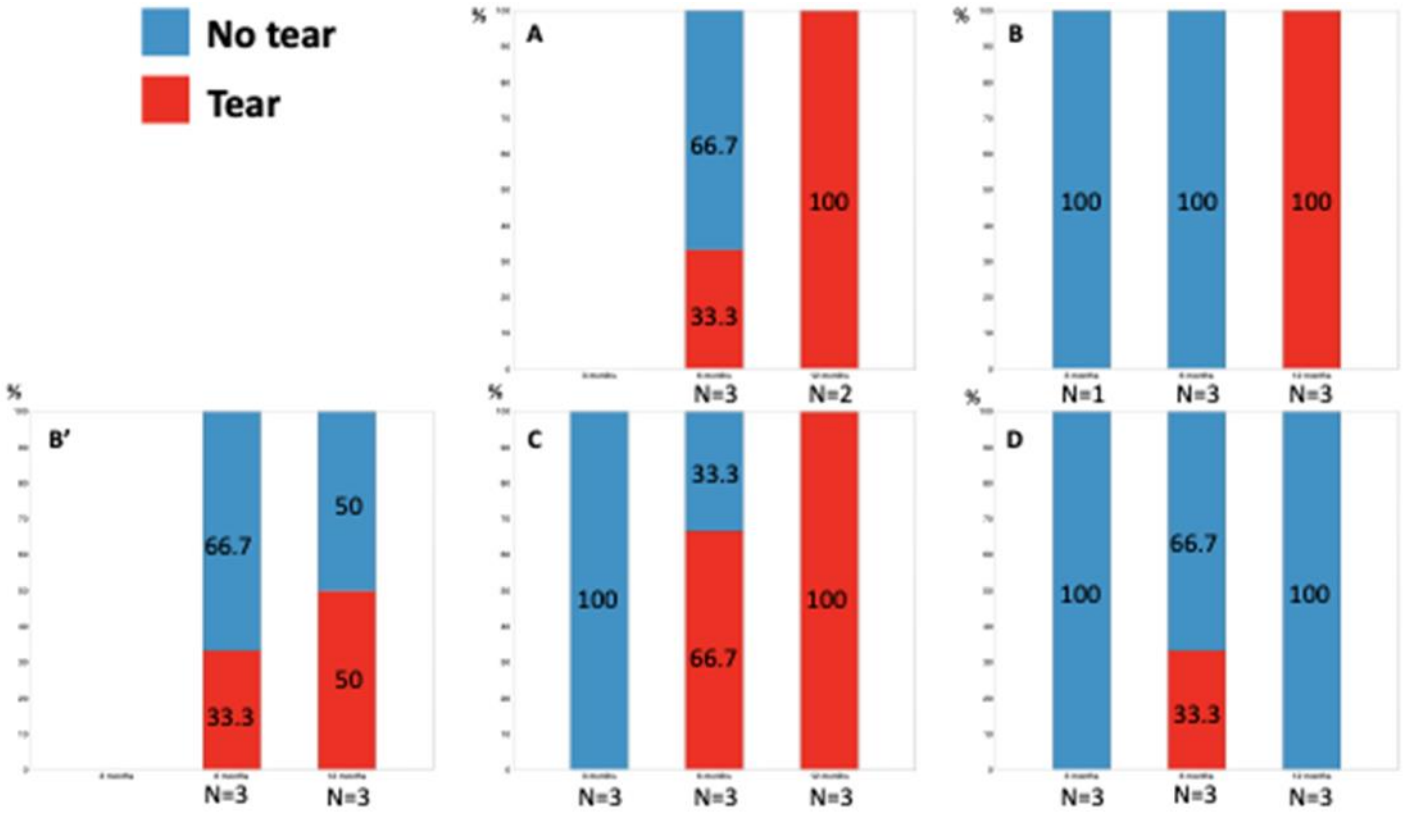

Supplementary Figure 5. Leaflet integrity assessment on radiographic images.

Leaflet gross pathology was classified into four categories (no tear [blue bar], tear [red bar]) by visual inspection and corroborated on radiographic images. This assessment was performed in the base, middle, and tip (free edge) of the leaflet of the five iterations at 3-, 6-, and 12-month follow-up.